Colloid Polym Sci (2004) 283: 243–249
DOI 10.1007/s00396-004-1087-2

ORIGINAL PAPER

Rong Guo
Zhongchun Li
Tianqing Liu

Catalysis of the electrochemical oxidation of L-cysteine by lyotropic mesophases

Received: 27 August 2003
Accepted: 15 January 2004
Published online: 19 October 2004

R. Guo (✉) · Z. Li · T. Liu
School of Chemistry and Chemical Engineering, Yangzhou University, 225002 Yangzhou, P.R. China
E-mail: guorong@yzu.edu.cn

Abstract The catalysis of the electrochemical oxidation of L-cysteine by sodium dodecyl sulfate (SDS)/benzyl alcohol (BA)/water (H_2O) lyotropic mesophases was studied by ultramicroelectrode cyclic voltammetry. The impact factors of catalysis on the electrochemical oxidation of L-cysteine depend on the structures, penetration and compositions of lyotropic liquid crystals. The catalytic efficiency η and rate constant k^0 increase with BA content at a constant mass ratio of SDS/H_2O, but decrease with SDS or water content at a constant mass ratio of BA/H_2O or SDS/BA in the lyotropic liquid crystals. The Gibbs free energy $\Delta G^{\neq}$ decreases with BA content at a constant mass ratio of SDS/H_2O, but increases with SDS or water content at a constant mass ratio of BA/H_2O or SDS/BA.

Keywords Sodium dodecyl sulfate · Lyotropic liquid crystals · Electrochemical oxidation · L-Cysteine · Catalysis

Introduction

L-Cysteine is widely applied in the fields of cosmetics, foodstuffs and pharmaceutical industries due to its greater resistance to oxidation, dough flexibility and treatment of hepatitis [1]. Lyotropic liquid crystals have characteristics of active cell membranes and can be regarded as model systems to simulate reactions in the life system, in which the physicochemical properties of bio-active reagents are investigated [2, 3, 4, 5, 6]. Investigations on the interactions between L-cysteine and molecular organized assemblies of surfactants are of significance for the preparation of biomaterials and molecular recognition.

The ultramicroelectrode technique, a new kind of electrochemical technique developed in recent years, has been extensively applied in electrochemistry, bioelectrochemistry and spectroelectrochemistry [7, 8, 9]. Ultramicroelectrodes have many unique characteristics compared with "normal" electrodes. For example, the time constant τ of the ultramicroelectrode is so small that it can be used to investigate fast transient electrochemical reactions. The low-polarized current on the ultramicroelectrode can decrease the ohmic potential drop, so that an ultramicroelectrode can be applied in high impendence systems such as solutions with or without supporting electrolytes, gases and also solid materials. Ultramicroelectrodes can also be used to determine the heterogeneous rate constants due to the fast mass transfer rate of electro-active reagents on the interface between the electrode and bulk solutions. In addition, the samples are not destroyed in the experiments due to the small electrode dimensions, so that ultramicroelectrodes can be applied in lyotropic mesophases. It can thus overcome the shortcomings of normal electrodes. In the present paper, ultramicroelectrode cyclic voltammetry is employed to investigate the interactions between L-cysteine and sodium dodecyl sulfate (SDS)/benzyl alcohol (BA)/water (H_2O) lyotropic mesophases, as well as the catalytic effect of lyotropic mesophases on the electrochemical oxidation of L-cysteine.

Materials and methods

Chemicals and materials

SDS (Sigma, 98%) was recrystallized twice in ethanol. The surface tension of the recrystallized product had no minimum around the critical micelle concentration (*cmc*) by the platinum ring method. L-cysteine (99%) was from Sigma, BA (99 + %) from Aldrich, potassium chloride (99%) from Sigma, and potassium ferrocyanide (99.5%) from Aldrich. Water used was twice distilled and deionized.

Experimental methods

Determination of partial phase diagram Samples were prepared in a test tube with a cap, mixed for several minutes, then placed in a thermostat at 25 ± 0.1 °C for at least 12 h for phase equilibrium. The phase boundaries of the lamellar liquid and hexagonal liquid crystals were determined with a polarizing microscope (59×, Shanghai Photology, China). Figure 1 illustrates the partial phase diagram of the SDS/BA/H_2O system. The dashed lines show the routes for determining the phases.

Preparation of ultramicroelectrode The ultramicroelectrode was fabricated by sealing a fine platinum wire with a radius of 10 μm in an insulator, such as a glass or plastic resin, and polished with super fine diamond paste and α-alumina particles of 0.05 μm size [10].

Determination of voltammetric properties of L-cysteine The voltammetric properties of L-cysteine were determined by a CHI660A potentiostat (Shanghai Chenhua, China). A three-electrode system was used with a platinum ultramicroelectrode as working electrode and a saturated calomel electrode (SCE) as reference electrode. The cyclic voltammograms were recorded from −0.4 V to 1.2 V versus SCE at 40 $mV \cdot s^{-1}$ potential sweep rate except the specified illustration. The electrodes were immersed in the samples for 5 min before measuring the voltammograms of L-cysteine. The reference electrode was kept in close proximity to the working electrode to minimize the ohmic drop.

Determination of Wuberg impendence The Wuberg impendence was determined using a Model 283 Potentiostat/Galvanostat and Model 5210 Lock-in Amplifier (EG & G, Princeton Applied Research, USA.). A three-electrode system was used with a platinum ultramicroelectrode as a working electrode and a SCE as a reference electrode. The frequency range was 100 kHz-10 mHz. The equilibrium time was 30 s.

Determination of the electrochemical catalytic efficiency The difficulty of electrochemical oxidation of L-cysteine is represented by the magnitude of the electrochemical oxidation current. At a given scan rate, the electrochemical catalytic efficiency is commonly defined as follows [11]:

$$\eta = \frac{i_a}{i_d} \quad (1)$$

where η is the catalytic efficiency, i_a and i_d are the anodic peak current with and without catalyst. i_a is the anodic peak current of L-cysteine in the liquid crystals, and i_d is the anodic peak current of 1.0×10^{-3} $mol \cdot L^{-1}$ L-cysteine in water.

All experiments were carried out at 25 ± 0.1 °C.

Results and discussion

The properties of the ultramicroelectrode

The diffusion coefficient of $Fe(CN)_6^{4-}$ calculated from the voltammetric equation was 6.3×10^{-6} $cm^2 \cdot s^{-1}$, which agrees with the reference value, 6.5×10^{-6} $cm^2 \cdot s^{-1}$ [12].

The electrochemical properties of L-cysteine

The cyclic voltammogram of 1.0×10^{-3} $mol \cdot L^{-1}$ L-cysteine is shown in Fig. 2. The anodic peak current and anodic

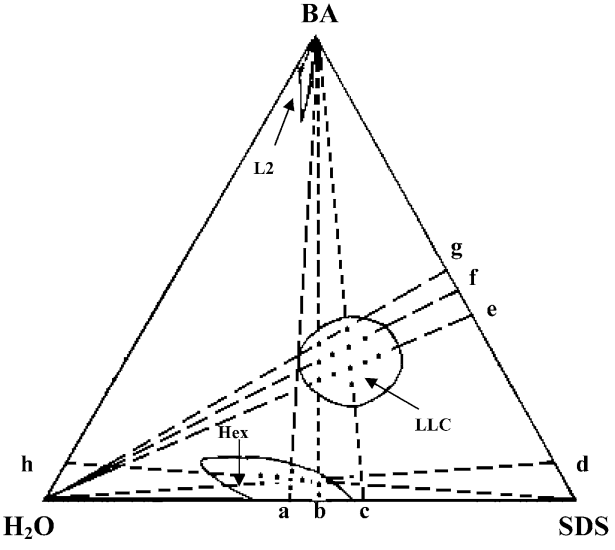

Fig. 1 Partial phase diagram of sodium dodecyl sulfate (*SDS*)/benzyl alcohol (*BA*)/H_2O system. Systems: *LLC* lamellar liquid crystals, *Hex* hexagonal liquid crystals. Mass ratios SDS/H_2O: *a* 45/55, *b* 55/45, *c* 60/40. Mass ratios SDS/BA: *d* 92/8, e—60/40, *f* 53/47, *g* 50/50. Mass ratio H_2O/BA: *h* 92/8

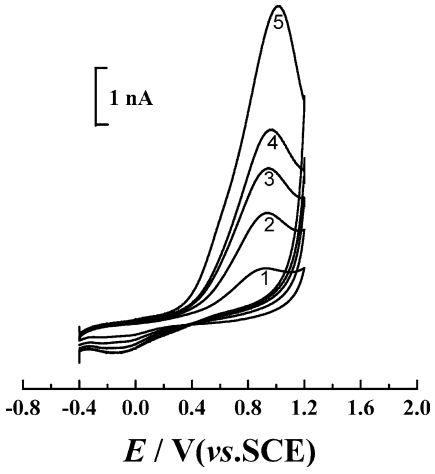

Fig. 2 Cyclic voltammogram at the different potential sweep rates for L-cysteine solution. Scan rate ($mV \cdot s^{-1}$): *1* 10, *2* 20, *3* 40, *4* 60, *5* 80. $C_{\text{L-cysteine}}$ ($mol \cdot L^{-1}$): 1.0×10^{-3}. *SCE* Saturated colomel electrode

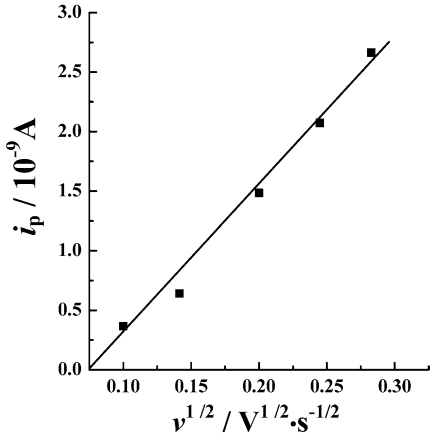

Fig. 3 Anodic peak current of L-cysteine as a function of the square root of the potential sweep rate

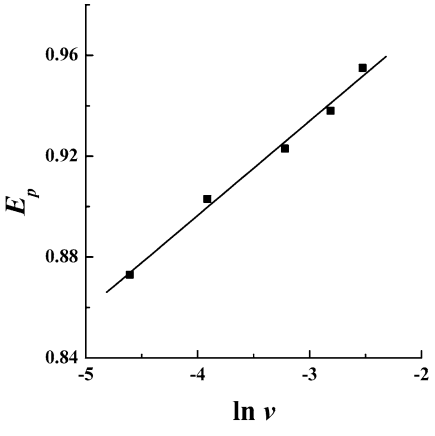

Fig. 4 Variation of the anodic peak potential E_p with the logarithm of scan rate. Correlation coefficient: $R = 0.995$

peak potential increase with the potential sweep rate, and the anodic peak current is proportional to the square root of the potential sweep rate (Fig. 3), which indicates that the electrode reaction of L-cysteine is diffusion-controlled and irreversible.

The relationship between the redox peak potential E_p and potential sweep rate v for an irreversible electrochemical reaction is:

$$E_p = E^{0'} - \frac{RT}{\alpha nF}\left[0.78 + \ln\left(\frac{D^{1/2}}{k^0}\right) + \ln\left(\frac{\alpha nFv}{RT}\right)^{1/2}\right] \quad (2)$$

where k^0 is the rate constant of electrode reaction, D the diffusion coefficient,and α the transfer coefficient. The apparent number of electron transfers ($\alpha n = 0.347$) is calculated from the linear relationship between E_p and ln v (Fig. 4).

The mechanism of electrochemical oxidation of L-cysteine in SDS/BA/H_2O lyotropic liquid crystals probably includes the following three steps:

$$RSH \leftrightarrow RSH(ads) \quad (3)$$

$$RSH(ads) \rightarrow RS(ads) + H^+ + e^- \quad (4)$$

$$2RS \leftrightarrow RSSR \quad (5)$$

where RSH is L-cysteine, RSSR is cystine, ads is SDS/BA/H_2O lyotropic liquid crystals absorbed on the surface of the electrode, and RS·(ads) are the radicals absorbed on the surface of the electrode. L-cysteine is solubilized in SDS/BA/H_2O lyotropic liquid crystals absorbed on the surface of the electrode as a transitional state, followed by the electrochemical reaction.

According to the theory of ultramicroelectrode [13, 14], the electrochemical reaction of L-cysteine on the platinum ultramicroelectrode can be described by

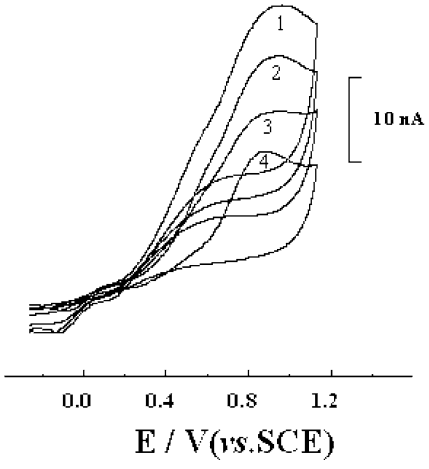

Fig. 5 Cyclic voltammogram for L-cysteine in the SDS/BA/H_2O lyotropic liquid crystals. Content of BA (%): *1* 37.5, *2* 34.2, *3* 29.6, *4* 25.7. All the lines on the voltammogram are from the 5th cycle

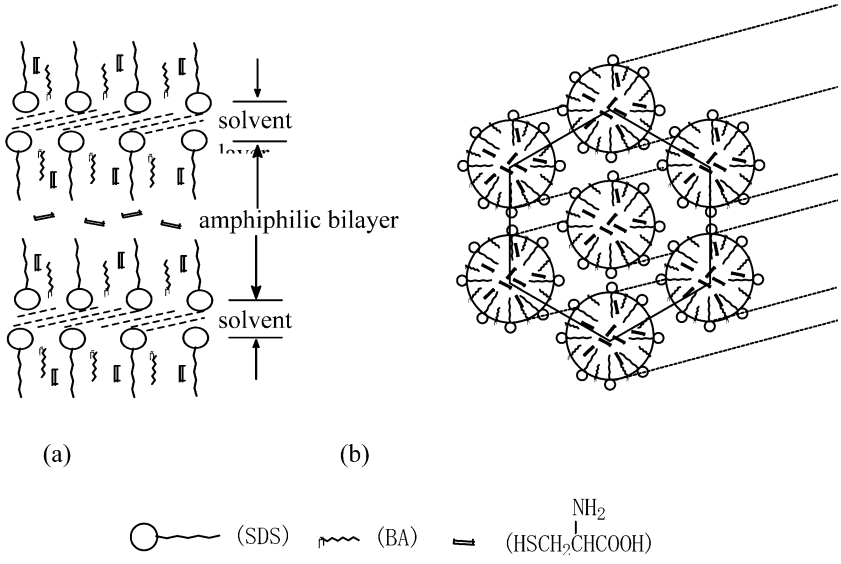

Fig. 6a, b Location of L-cysteine in SDS/BA/H_2O lyotropic liquid crystals. **a** Lamellar liquid crystals. **b** Hexagonal liquid crystals

$$i_p = 4\alpha nFDrC\left[0.34\exp.(-0.66P) + 0.66 - 0.13\exp\left(-\frac{11}{P}\right) + 0.351P\right] \quad (6)$$

where i_p is the anodic peak current, F the Faraday constant, C the concentration of electro-active reagent, r the radius of ultramicroelectrode. n is the number of electrons involved in the electrode reaction, D is the diffusion coefficient, and P is a characteristic parameter of the ultramicroelectrode:

$$P = \left(\frac{\alpha nFr^2 v}{RTD}\right)^{\frac{1}{2}} \quad (7)$$

where v is the potential sweep rate, T the absolute temperature, and R the gas constant. The diffusion coefficient of L-cysteine was calculated from Eq. 6 and Eq. 7 by the Newton iteration method.

Catalysis by lyotropic liquid crystals

The cyclic voltammogram of L-cysteine in the lyotropic liquid crystals is shown in Fig. 5. The anodic peak current is larger than that in the aqueous solution (Fig. 2) at the same concentration and potential sweep rate. This indicates that the electrochemical oxidation of L-cysteine in the lyotropic liquid crystals proceeds more easily than in the aqueous solution at the same concentration. As

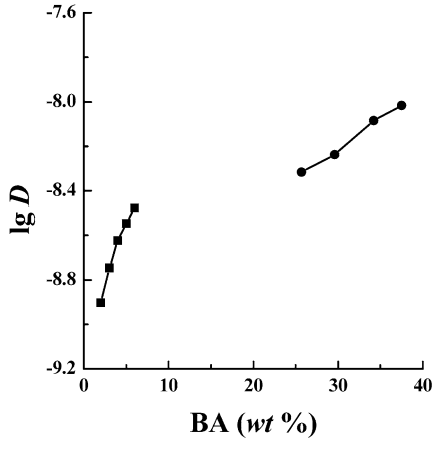

Fig. 7 Diffusion coefficient of L-cysteine with the content of BA at different mass ratios of SDS/H_2O. Systems: *squares* hexagonal liquid crystals, *circles* lamellar liquid crystals. Mass ratios SDS/H_2O: *squares* 45/55,*circles* 60/40

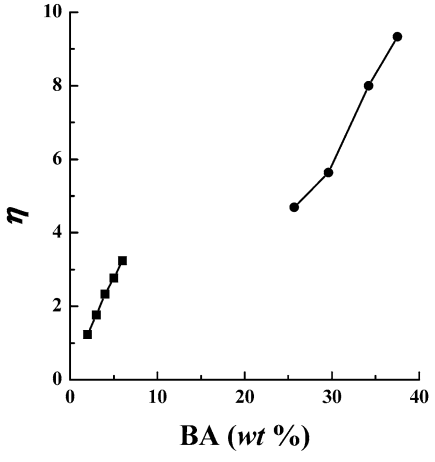

Fig. 8 Catalytic efficiency with the content of BA at different mass ratios of SDS/H_2O. Systems: *squares* hexagonal liquid crystals, *circles* lamellar liquid crystals. Mass ratios SDS/H_2O: *squares* 45/55,*circles* 60/40

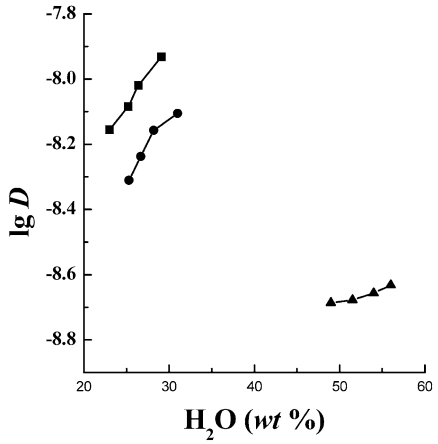

Fig. 9 Diffusion coefficient of L-cysteine with the content of water at different mass ratios of SDS/BA. Systems: *squares*, *circles* lamellar liquid crystals, *triangles* hexagonal liquid crystals. Mass ratios SDS/BA:*squares* 53/47, *circles* 60/40, *triangles* 92/8

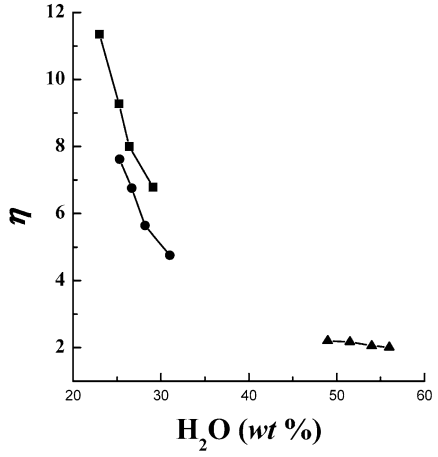

Fig. 10 Catalytic efficiency with the content of water at different mass ratios of SDS/BA. Systems: *squares*, *circles* lamellar liquid crystals, *triangles* hexagonal liquid crystals. Mass ratios SDS/BA: *squares*— 53/47, *circles* 60/40, *triangles* 92/8

the increase in the diffusion coefficient can increase the peak current, the electrochemical reaction rate can be evaluated by electrochemical reaction current. Therefore, the increase of anodic peak current of L-cysteine indicates an increase in the electrochemical oxidation rate of L-cysteine, which reveals the catalytic effect of the liquid crystals. Figure 6 shows the insertion of L-cysteine in the lamellar and hexagonal liquid crystals. The L-cysteine can be solubilized in the amphiphilic bilayer of the lamellar liquid crystals and the inner core of the hexagonal liquid crystals. The solubilization of L-cysteine by the liquid crystals increases the concentration of L-cysteine on the electrode surface, which increases the anodic peak current.

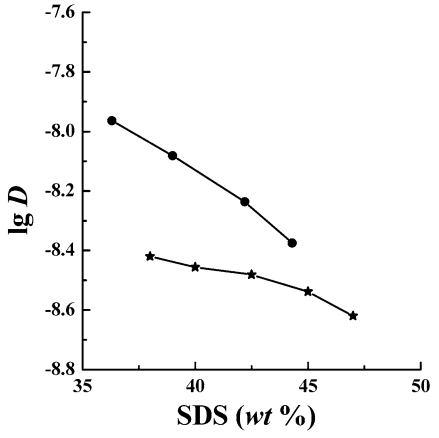

Fig. 11 Diffusion coefficient of L-cysteine with the content of SDS at different mass ratios of H_2O/BA. Systems: *stars* hexagonal liquid crystals, *circles* lamellar liquid crystals. Mass ratios: *stars* H_2O/BA = 92/8, *circles* H_2O/BA = 50/50

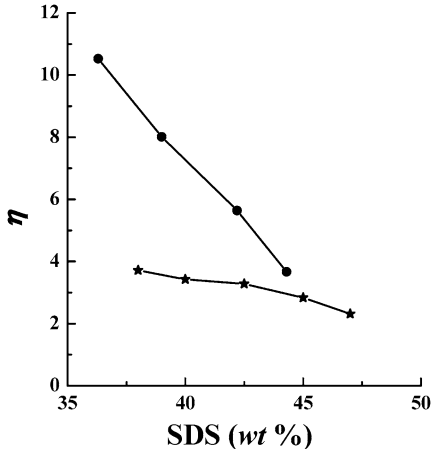

Fig. 12 Catalytic efficiency with the content of SDS at different mass ratios of H_2O/BA. Systems: *stars* hexagonal liquid crystals, *circles* lamellar liquid crystals. Mass ratios: *stars* H_2O/BA = 92/8, *circles* H_2O/BA = 50/50

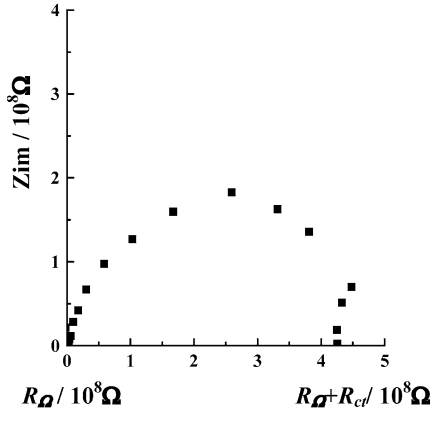

Fig. 13 Plots of Wuberg impendence for L-cysteine. $C_{\text{L-cysteine}}$ (mol·L^{-1}): 1.0×10^{-3}

Table 1 Rate constant k^0 and Gibbs free energy $\Delta G^{\neq}$ in the SDS/BA/H_2O lamellar liquid crystals. k^0 and $\Delta G^{\neq}$ units are 10^{-4} cm·s^{-1}and kJ·mol^{-1}, respectively

$W_{SDS}/W_{BA}=53/47$			$W_{SDS}/W_{BA}=60/40$			$W_{SDS}/W_{H2O}=45/55$			$W_{H2O}/W_{BA}=92/8$		
W_{H2O}%	k^0	$\Delta G^{\neq}$	W_{H2O}%	k^0	$\Delta G^{\neq}$	W_{BA}%	k^0	$\Delta G^{\neq}$	W_{SDS}%	k^0	$\Delta G^{\neq}$
29.1	11.08	101.30	31.0	7.758	102.19	37.5	15.24	100.51	38.0	6.071	102.80
26.4	13.06	100.90	28.2	9.202	101.76	34.2	13.06	100.90	40.0	5.590	103.00
25.2	15.15	100.53	26.7	11.03	101.32	29.6	9.202	101.76	42.5	5.355	103.11
23.0	18.54	100.03	25.3	12.45	101.02	25.7	7.655	102.22	45.0	4.631	103.47
-	-	-	-	-	-	-	-	-	47.0	3.777	103.97

Table 2 Rate constant k^0 and Gibbs free energy $\Delta G^{\neq}$ in the SDS/BA/H_2O hexagonal liquid crystals

$W_{SDS}/W_{H2O}=45/55$			$W_{SDS}/W_{BA}=92/8$		
W_{BA}%	$k^0/10^{-4}$ cm·s^{-1}	$\Delta G^{\neq}$ /KJ·mol^{-1}	W_{H2O}%	$k^0/10^{-4}$ cm·s^{-1}	$\Delta G^{\neq}$ /kJ·mol^{-1}
2.0	2.007	105.54	49.0	3.589	104.10
3.0	2.868	104.65	51.5	3.535	105.35
4.0	3.802	103.96	54.0	3.357	105.48
5.0	4.520	103.54	56.0	3.286	105.53
6.0	5.296	103.13	-	-	-

The effects of BA content

BA is located in the amphiphilic bilayer as a cosurfactant [15]. The spacing between SDS molecules in the amphiphilic bilayer increases with the addition of BA content at a constant mass ratio of SDS/H_2O, which increases the diffusion coefficient of L-cysteine (Fig. 7). Therefore, the catalytic efficiency is increased by the addition of BA (Fig. 8).

Water content and catalytic efficiency

Some of the water molecules in lamellar liquid crystal lie in the solvent layer and the others penetrate into the amphiphilic bilayer. Thus, the distance of the SDS molecules in the bilayer and the amount of water increase with the addition of water at a constant mass ratio of SDS/BA, and the increase of the diffusion coefficient of L-cysteine in the lamellar liquid crystals (Fig. 9). On the other hand, the actual concentration of L-cysteine decreases with the water content, decreasing the anodic peak current of L-cysteine. So the catalytic efficiency decreases with increasing water content at a constant mass ratio of SDS/BA (Fig. 10).

SDS content and catalytic efficiency

Obviously, the increase of the SDS content at a constant mass ratio of BA/H_2O causes a closer structure of the amphiphilic bilayer, which reduces the diffusion coefficient of L-cysteine (Fig. 11). Thus, the catalytic efficiency and anodic peak current decrease (Fig. 12).

Catalysis of the electrochemical oxidation of L-cysteine by the hexagonal mesophases

For the hexagonal liquid crystals, the catalytic efficiency and diffusion coefficient increase with the addition of BA at a constant mass ratio of SDS/H_2O (Fig. 7, Fig. 8). At a constant mass ratio of SDS/BA or BA/H_2O, the catalytic efficiency and diffusion coefficient decrease with the content of water or SDS. Because of the closer structure and higher viscosity of hexagonal liquid crystals, the diffusion coefficient of L-cysteine is less than that in lamellar liquid crystals (Fig. 7, Fig. 9, Fig. 11). Thus, the catalytic efficiency by hexagonal liquid crystals is lower than that by lamellar liquid crystals (Fig. 8, Fig. 10, Fig. 12).

In addition, the range of catalytic efficiency with BA content at a constant mass ratio of SDS/H_2O in hexagonal liquid crystals is larger than for lamellar liquid crystals, but the range of catalytic efficiency with water or SDS content at a constant mass ratio of SDS/BA or BA/H_2O is lower in hexagonal liquid crystals than in lamellar liquid crystals. Obviously, this result is related to the three-dimensional structures of BA, water and SDS molecules. The effects of BA content on the diffusion coefficient of L-cysteine in the closer structure of hexagonal liquid crystals is greater than in lamellar liquid crystal due to the larger three-dimensional structure of BA molecules (Fig. 7). However, the effects of water or SDS content on the diffusion coefficient of L-cysteine in hexagonal liquid crystals are smaller than in lamellar liquid crystals due to the smaller three-dimensional structure of water or SDS molecules (Fig. 9, Fig. 11).

Rate constant k^0 and Gibbs free energy $\Delta G^{\neq}$

The exchange current i_0, rate constant k^0 and charge-transfer resistance R_{ct} obey the equations [16]:

$$R_{ct} = \frac{RT}{nFi_0} \tag{8}$$

$$\frac{RT}{nFR_{ct}} = nFAk^0C_R \tag{9}$$

$$k^0 = \frac{RT}{n^2F^2AC_RR_{ct}} \tag{10}$$

The charge-transfer resistance R_{ct} is obtained from the plots of Wuberg impendence (Fig. 13). The rate constant k^0 can easily be calculated from Eq. 10 and the results are listed in Table 1 and Table 2. The rate constant k^0 increases with BA content at a constant mass ratio of SDS/H_2O, but decreases with SDS or water content at a constant mass ratio of BA/H_2O or SDS/BA.

According to the mechanism of electrochemical oxidation of L-cysteine and the theory of transition state [17], we have

$$k^0 = \frac{k_BT}{h}\exp\left(\frac{-\Delta G^{\neq}}{RT}\right) \tag{11}$$

$$\Delta G^{\neq} = -RT\ln\left(\frac{k^0h}{k_BT}\right) \tag{12}$$

where $\Delta G^{\neq}$ is the Gibbs free energy of the electrode reaction and is a function related to the electric field, k_B the Boltzmann constant, and h the Plank constant. The Gibbs free energy $\Delta G^{\neq}$ can be obtained from Eq. 12 (Table 1, Table 2). The Gibbs free energy $\Delta G^{\neq}$ decreases with the BA content at a constant mass ratio of SDS/H_2O, but increases with the SDS or water content at a constant mass ratio of BA/H_2O or SDS/BA. The results also indicate that the electrochemical oxidation of L-cysteine is catalyzed by the lyotropic mesophases.

Conclusions

The reaction of electrochemical oxidation of L-cysteine on the platinum ultramicroelectrode is diffusion-controlled and irreversible. In the SDS/BA/H_2O lyotropic mesophases, the catalytic efficiency η and rate constant k^0 increase with BA content at a constant mass ratio of SDS/H_2O, but decrease with SDS or water content at a constant mass ratio of BA/H_2O or SDS/BA. However, the Gibbs free energy $\Delta G^{\neq}$ decreases with BA content at a constant mass ratio of SDS/H_2O, but increases with SDS or water content at a constant mass ratio of BA/H_2O or SDS/BA.

Acknowledgements This work was supported by the National Nature Science Foundation of China. (No.20073038 & 20233010)

References

1. Ralph TR, Hitchman ML, Millington JP, Walsh FC (1994) J Electroanal Chem 375:1
2. Guo R, Friberg SE (1991) Acta Biochim Biophys Sin 23:89
3. Pesavento M, Profumo A (1991) Talanta 38:1099
4. Guo R, Liu TQ, Yu WL (1999) Langmuir 15:624
5. Guo R, Fan GK, Liu TQ (2000) Acta Chim Sin 58:636
6. Fendler J H (1982) Membrane mimetic chemistry. Wiley, New York, pp 1–52
7. Osamu N, Hisao T (1994) Anal Chem 66:285
8. Ellie AG, Willson AM, Tour JM, Brockmann TW, Zhang P, Allara DL (1995) Langmuir 11:1768
9. Gregoryt AK, Petersen K (1996) Anal Chem News Features 7:407
10. Xu JX, Liu TQ, Guo R (2003) Acta Phys Chim Sin 19:364
11. Andrienx CP, Blocman C, Duas-Bouchiat JM, Halla FM, Saveant JM (1980) J Electroanal Chem 113:19
12. Stackelberg MV, Pligram M, Toome W (1953) Z Elektrochem 57:342
13. Aoki K, Akimoto K, Tokuda K, Matsuda H (1984) J Electroanal Chem 171:219
14. Bard AJ, Fan FR, Juhyoun K, Ovadia L (1989) Anal Chem 61:132
15. Guo R, Mary EC, Friberg SE (1996) J Disp Sci Technol 17:493
16. Bard A J, Larry R F (2001) Electrochemical methods: fundamentals and applications. Wiley, New York, pp 174, 236
17. Zhao ZG, Shen JJ, Ma JM (2003) Acta Chim Sin 61:298